

Fermi and non-Fermi Liquid Behavior in Quantum Impurity Systems: Conserving Slave Boson Theory

Johann Kroha and Peter Wölfle

Institut für Theorie der Kondensierten Materie, Universität Karlsruhe
D-76128 Karlsruhe, Germany

Summary: We review a recently developed method, based on an exact auxiliary boson representation, to describe both Fermi liquid and non-Fermi liquid behavior in quantum impurity systems. Coherent spin and charge fluctuation processes are taken into account in a self-consistent way and are shown to include *all* leading and subleading infrared singularities at any given order of the self-consistent loop expansion of the free energy. As a consequence, for the $SU(N) \times SU(M)$ Anderson impurity models the correct temperature dependence of the susceptibility is recovered over the entire temperature range, including Fermi liquid or non-Fermi liquid behavior below the Kondo temperature T_K . As a standard diagram technique the presented method has the potential to be generalized to correlated electron systems on a lattice.

1 Introduction

Highly correlated electron systems are characterized by a strong repulsion between electrons on the same lattice site, effectively restricting the dynamics to the Fock subspace of states without double occupancy of sites. The prototype model for such systems is the Anderson impurity model, which consists of an electron in a localized level $\varepsilon_d < 0$ (called d-level in the following) with on-site repulsion U , hybridizing via a transition matrix element V with one or several degenerate conduction electron bands or channels [1]. Depending on the number of channels M , the model exhibits the single- or the multi-channel Kondo effect, where at temperatures T below the Kondo temperature T_K the local electron spin is screened ($M = 1$) or overscreened ($M \geq 2$) by the conduction electrons, leading to Fermi liquid (FL) or to non-Fermi liquid (NFL) behavior [2] with characteristic low-temperature singularities, respectively.

As perhaps the simplest model to investigate the salient features of correlations induced by short-range repulsion, the Anderson model plays a central role for the description of strongly correlated electron systems: In the limit of large

spatial dimensions [3] strongly correlated lattice systems reduce in general to a single Anderson impurity hybridizing with a continuum of conduction electron states whose properties are determined from a self-consistency condition imposed by the translational invariance of the system [4]. Quantum impurity models have received further interest due to their relevance for mesoscopic systems like single electron transistors or quantum point contacts [5]. Nonlinear conductance anomalies observed in the latter systems [6] have provided one of the strongest cases for the physical realization of the two-channel Kondo effect generated by two-level systems with electron assisted tunneling.

The above-mentioned systems call for the development of accurate and flexible theoretical methods, applicable to situations where exact solution methods are not available. We here present a general, well-controlled auxiliary boson technique which correctly describes the FL as well as the NFL case of the generalized $SU(N) \times SU(M)$ Anderson impurity model. As a standard diagram technique it has the potential to be generalized for correlated lattice problems as well as for non-equilibrium situations in mesoscopic systems.

In section 2 we describe several exact properties of the auxiliary particle representation, while the conserving slave boson theory is developed and evaluated in section 3.

2 Exact Auxiliary Particle Representation

2.1 The $SU(N) \times SU(M)$ Anderson Impurity Model

The auxiliary or slave boson method [7] is a powerful tool to implement the effective restriction to the sector of Fock space with no double occupancy imposed by a large on-site repulsion U . The creation operator for an electron with spin σ in the d -level is written in terms of fermionic operators f_σ and bosonic operators b as $d_\sigma^\dagger = f_\sigma^\dagger b$. This representation is exact, if the constraint that the total number operator of auxiliary fermions f_σ and bosons b is equal to unity is obeyed. f_σ^\dagger and b^\dagger may be envisaged as creating the three allowed states of the impurity: singly occupied with spin σ or empty.

In view of the possibility of both FL and NFL behavior in quantum impurity systems mentioned in the introduction it is useful to introduce M degenerate channels for the conduction electron operators $c_{\sigma\mu}^\dagger$, labeled $\mu = 1, 2, \dots, M$, in such a way that in the limit of impurity occupation number $n_d \rightarrow 1$ (Kondo limit) the M -channel Kondo model is recovered, i.e. the model obeys an $SU(M)$ channel symmetry. The slave bosons then form an $SU(M)$ multiplet $b_{\bar{\mu}}$ which transforms according to the conjugate representation of $SU(M)$, so that μ is a conserved quantum number. Generalizing, in addition, to arbitrary spin degeneracy N ,

$\sigma = 1, 2, \dots, N$, one obtains the $SU(N) \times SU(M)$ Anderson impurity model in slave boson representation

$$H = \sum_{\vec{k}, \sigma, \mu} \varepsilon_{\vec{k}} c_{\vec{k}\mu\sigma}^\dagger c_{\vec{k}\mu\sigma} + E_d \sum_{\sigma} f_{\sigma}^\dagger f_{\sigma} + V \sum_{\vec{k}, \sigma, \mu} (c_{\vec{k}\mu\sigma}^\dagger b_{\mu}^\dagger f_{\sigma} + h.c.), \quad (2.1)$$

where the local operator constraint $\hat{Q} \equiv \sum_{\sigma} f_{\sigma}^\dagger f_{\sigma} + \sum_{\mu} b_{\mu}^\dagger b_{\mu} = 1$ must be fulfilled at all times.

2.2 Gauge Symmetry and Exact Projection onto the Physical Fock Space

The system described by the auxiliary particle Hamiltonian (2.1) is invariant under simultaneous, local $U(1)$ gauge transformations, $f_{\sigma} \rightarrow f_{\sigma} e^{i\phi(\tau)}$, $b_{\bar{\mu}} \rightarrow b_{\bar{\mu}} e^{i\phi(\tau)}$, with $\phi(\tau)$ an arbitrary, time dependent phase. While the gauge symmetry guarantees the conservation of the local, integer charge Q , it does not single out any particular Q , like $Q = 1$. In order to effect the projection onto the $Q = 1$ sector of Fock space, one may use the following procedure [8, 9]: Consider first the grand-canonical ensemble with respect to Q and the associated chemical potential $-\lambda$. The expectation value in the $Q = 1$ subspace of any physical operator \hat{A} acting on the impurity states is then obtained as

$$\langle \hat{A} \rangle = \lim_{\lambda \rightarrow \infty} \frac{\frac{\partial}{\partial \zeta} \text{tr}[\hat{A} e^{-\beta(H+\lambda Q)}]_G}{\frac{\partial}{\partial \zeta} \text{tr}[e^{-\beta(H+\lambda Q)}]_G} = \lim_{\lambda \rightarrow \infty} \frac{\langle \hat{A} \rangle_G}{\langle Q \rangle_G}, \quad (2.2)$$

where the index G denotes the grand canonical ensemble and ζ is the fugacity $\zeta = e^{-\beta\lambda}$. In the second equality of Eq. (2.2) we have used the fact that any physical operator \hat{A} acting on the impurity is composed of the impurity electron operators d_{σ} , d_{σ}^\dagger , and thus annihilates the states in the $Q = 0$ sector, $\hat{A}|Q = 0\rangle = 0$. It is obvious that the grand-canonical expectation value involved in Eq. (2.2) may be factorized into auxiliary particle propagators using Wick's theorem, thus allowing for the application of standard diagrammatic techniques.

It is important to note that, in general, λ plays the role of a time dependent gauge field. In Eq. (2.2) a time independent gauge for λ has been chosen. In this way, the projection is only performed at one instant of time, explicitly exploiting the conservation of the local charge Q . Thus, choosing the time independent gauge means that in the subsequent development of the theory, the Q conservation must be implemented exactly. This is achieved in a systematic way by means of conserving approximations [10], i.e. by deriving all self-energies and vertices by functional derivation from one common Luttinger-Ward functional Φ of the fully renormalized Green's functions,

$$\Sigma_{b,f,c} = \delta\Phi\{G_b, G_f, G_c\}/\delta G_{b,f,c}. \quad (2.3)$$

This amounts to calculating all quantities of the theory in a self-consistent way, but has the great advantage that gauge field fluctuations need not be considered.

2.3 Infrared Threshold Behavior of Auxiliary Propagators

The projection onto the physical subspace, Eq. (2.2), implies that the pseudo-fermion and slave boson Green's functions G_f, G_b are defined as the usual time-ordered, grand canonical expectation values of a pair of creation and annihilation operators, however evaluated in the limit $\lambda \rightarrow \infty$. It follows that the traces involved in G_f, G_b are taken purely over the the $Q = 0$ sector of Fock space, and thus the backward-in-time contribution to the auxiliary particle propagators vanishes. Consequently, the auxiliary particle propagators are formally identical to the core hole propagators appearing in the well-known X-ray problem [11], and the long-time behavior of G_f (G_b) is determined by the orthogonality catastrophe [12] of the overlap of the Fermi sea without impurity ($Q = 0$) and the fully interacting conduction electron sea in the presence of a pseudofermion (slave boson) ($Q = 1$). It may be shown that the auxiliary particle spectral functions have threshold behavior with vanishing spectral weight at $T = 0$ for energies ω below a threshold E_o , and power law behavior above E_o , $A_{f,b}(\omega) \propto \Theta(\omega - E_o)\omega^{-\alpha_{f,b}}$.

For the single-channel Anderson model, which is known to have a FL ground state, the threshold exponents may be deduced from an analysis in terms of scattering phase shifts, using the Friedel sum rule, since in the spin screened FL state the impurity acts as a pure potential scatterer [13, 14, 15, 16],

$$\alpha_f = \frac{2n_d - n_d^2}{N}, \quad \alpha_b = 1 - \frac{n_d^2}{N} \quad (N \geq 1, M = 1) \quad (2.4)$$

These results have been confirmed by numerical renormalization group (NRG) calculations [17] and by use of the Bethe ansatz solution in connection with boundary conformal field theory (CFT) [18]. On the contrary, in the NFL case of the multi-channel Kondo model the threshold exponents have been deduced by a CFT solution [19] as

$$\alpha_f = \frac{M}{M + N}, \quad \alpha_b = \frac{N}{M + N} \quad (N \geq 2, M \geq N) \quad (2.5)$$

Since the dependence of α_f, α_b on the impurity occupation number n_d shown above originates from pure potential scattering, it is characteristic for the FL case. The auxiliary particle threshold exponents are, therefore, indicators for FL or NFL behavior in quantum impurity models of the Anderson type.

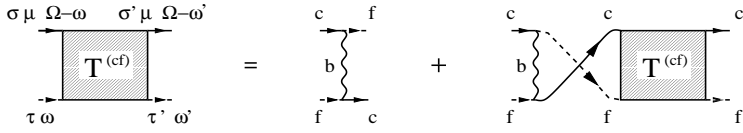


Figure 1 Diagrammatic representation of the Bethe–Salpeter equation defining the conduction electron–pseudofermion T-matrix $T^{(cf)}$.

3 Conserving Slave Particle T-Matrix Approximation

3.1 Non-Crossing Approximation (NCA)

The conserving formulation discussed in section 2.2 precludes mean field approximations which break the $U(1)$ gauge symmetry, like slave boson mean field theory. Although the latter can in some cases successfully describe the low T behavior of models with a FL ground state, it leads to a spurious phase transition at finite T and, in particular, fails to describe NFL systems.

Rather, the approximation should be generated from a Luttinger-Ward functional Φ . Using the hybridization V as a small parameter, one may generate successively more complex approximations. The lowest order conserving approximation generated in this way is the Non-crossing Approximation (NCA) [20, 21], defined by the first diagram in Fig. 2, labeled “NCA”. The NCA is successful in describing Anderson type models at temperatures above and around the Kondo temperature T_K , and even reproduces the threshold exponents Eq. (2.5) for the NFL case of the Anderson impurity model. However, it fails to describe the FL regime at low temperatures. This may be traced back to the failure to capture the spin-screened Kondo singlet ground state of the model, since coherent spin flip scattering is not included in NCA, as seen below.

3.2 Dominant Contributions at Low Energy

In order to eliminate the shortcomings of the NCA mentioned above, we may use as a guiding principle to look for contributions to the vertex functions which renormalize the auxiliary particle threshold exponents to their correct values, since this is a necessary condition for the description of FL and NFL behavior, as discussed in section 2.3. As shown by power counting arguments [22], there are no corrections to the NCA exponents in any finite order of perturbation theory. Thus, any renormalization of the NCA exponents must be due to singularities arising from an infinite resummation of terms. In general, the existence of collective excitations leads to a singular behavior of the corresponding two-particle vertex function. In view of the tendency of Kondo systems to form a collective spin singlet state, we expect a singularity in the spin singlet channel

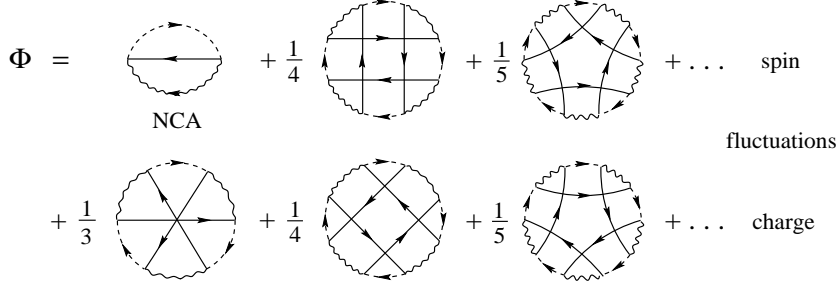


Figure 2 Diagrammatic representation of the Luttinger-Ward functional generating the CTMA. The terms with the conduction electron lines running clockwise (labelled “spin fluctuations”) generate $T^{(cf)}$, while the terms with the conduction electron lines running counter-clockwise (labelled “charge fluctuations”) generate $T^{(cb)}$. The two-loop diagram is excluded, because it is not a skeleton.

of the pseudofermion–conduction electron vertex function. It is then natural to perform a partial resummation of those contributions which, at each order in the hybridization V , contain the maximum number of spin flip processes. This amounts to calculating the conduction electron–pseudofermion vertex function in the “ladder” or T-matrix approximation, $T^{(cf)}$, where the irreducible vertex is given by $V^2 G_b$. The Bethe–Salpeter equation for $T^{(cf)}$ reads (Fig. 1),

$$\begin{aligned}
 T_{\sigma\tau,\sigma'\tau'}^{(cf)\mu}(i\omega_n, i\omega'_n, i\Omega_n) = & + V^2 G_{b\bar{\mu}}(i\omega_n + i\omega'_n - i\Omega_n) \delta_{\sigma\tau'} \delta_{\tau\sigma'} \\
 & - V^2 T \sum_{\omega''_n} G_{b\bar{\mu}}(i\omega_n + i\omega''_n - i\Omega_n) \times \\
 & G_{f\sigma}(i\omega''_n) G_{c\mu\tau}^0(i\Omega_n - i\omega''_n) T_{\tau\sigma,\sigma'\tau'}^{(cf)\mu}(i\omega''_n, i\omega'_n, i\Omega_n),
 \end{aligned} \tag{3.6}$$

where $\sigma, \tau, \sigma', \tau'$ represent spin indices and μ a channel index. A similar integral equation holds for the charge fluctuation T-matrix $T^{(cb)}$; it is obtained from $T^{(cf)}$ by interchanging $f_\sigma \leftrightarrow b_\mu$ and $c_{\sigma\mu} \leftrightarrow c_{\sigma\mu}^\dagger$. Inserting NCA Green’s functions for the intermediate state propagators of Eq. (3.6), we find at low temperatures and in the Kondo regime ($n_d \gtrsim 0.7$) a pole of $T^{(cf)}$ in the singlet channel as a function of the center-of-mass (COM) frequency Ω , at a frequency which scales with the Kondo temperature, $\Omega = \Omega_{cf} \simeq -T_K$. Similarly, the corresponding T-matrix $T^{(cb)}$ in the conduction electron–slave boson channel, evaluated within the analogous approximation, develops a pole at negative values of Ω in the empty orbital regime ($n_d \lesssim 0.3$). In the mixed valence regime ($n_d \simeq 0.5$) the poles in both $T^{(cf)}$ and $T^{(cb)}$ coexist. The appearance of poles in the two-particle vertex functions $T^{(cf)}$ and $T^{(cb)}$, which signals the formation of collective states, may be expected to influence the behavior of the system in a major way.

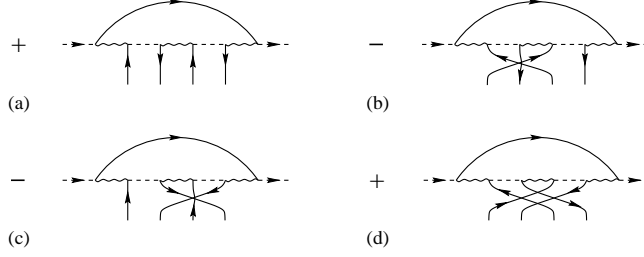


Figure 3 Set of skeleton diagram parts *not* contained in CTMA which cancel in the infrared limit to leading and subleading order in the external frequency, $\omega \rightarrow 0$.

3.3 Self-consistent Formulation

The approximation considered so far is not yet consistent: The spectral weight produced by the poles of $T^{(cf)}$ and $T^{(cb)}$ at negative frequencies Ω is strictly prohibited in the limit $T \rightarrow 0$ by the threshold property of auxiliary particle vertex functions (compare section 2.3). However, recall that a minimum requirement on the approximation used is the conservation of gauge symmetry. This requirement is not met when the integral kernel of the T -matrix equation is approximated by the NCA result. Rather, the approximation should be generated from the Luttinger-Ward functional shown in Fig. 2. It is defined as the infinite series of all vacuum skeleton diagrams which consist of a single ring of auxiliary particle propagators, where each conduction electron line spans at most two hybridization vertices. The first diagram of the infinite series of CTMA terms corresponds to NCA. By functional differentiation with respect to the conduction electron Green's function and the pseudofermion or the slave boson propagator, respectively, the shown Φ functional generates the ladder approximations $T^{(cf)}$, $T^{(cb)}$ for the total conduction electron-pseudofermion vertex function and for the total conduction electron-slave boson vertex function (Fig. 1). The auxiliary particle self-energies are obtained in the conserving scheme as the functional derivatives of Φ with respect to G_f or G_b , respectively (Eq. (2.3)), and are, in turn, non-linear functionals of the full, renormalized auxiliary particle propagators. This defines a set of self-consistency equations, which we term conserving T -matrix approximation (CTMA).

The CTMA is justified on formal grounds by a cancellation theorem for all diagrams not included in the generating functional Φ [16]: As seen in Fig. 2, Φ includes *all* contributions where a conduction electron line spans up to two hybridization vertices; contributions not included contain at least one conduction electron arch spanning four vertices. These contributions cancel pairwise at arbitrary loop order to leading and subleading order in the external frequency, as illustrated in Fig. 3.

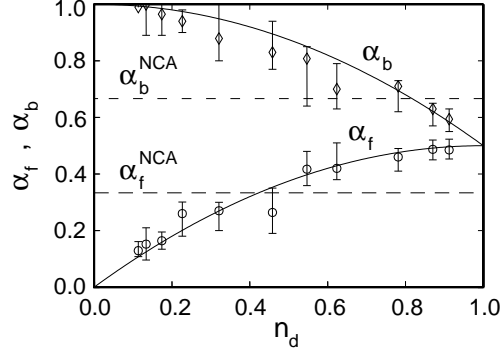


Figure 4 The fermion and boson threshold exponents α_f , α_b are shown for $N = 2$, $M = 1$ in dependence of the average impurity occupation n_d . Solid lines: exact values, Eq. (2.4); Symbols with error bars: CTMA; dashed lines: NCA.

3.4 Results

We have solved the CTMA equations numerically for a wide range of impurity occupation numbers n_d from the Kondo to the empty impurity regime both for the single-channel and for the two-channel Anderson model down to temperatures of the order of at least $10^{-2}T_K$.

The solution of the CTMA equations forces the T-matrices to have vanishing spectral weight at negative COM frequencies Ω . Indeed, the numerical evaluation shows that the poles of $T^{(cf)}$ and $T^{(cb)}$ are shifted to $\Omega = 0$ by self-consistency, where they merge with the continuous spectral weight present for $\Omega > 0$, and thus renormalize the threshold exponents of the auxiliary spectral functions. For $N = 2$, $M = 1$ the threshold exponents α_f , α_b extracted from the numerical solutions are shown in Fig. 4. In the Kondo limit of the multi-channel case ($N \geq 2$, $M = 2, 4$) the CTMA solutions are found not to alter the NCA values and reproduce the the correct threshold exponents, $\alpha_f = M/(M + N)$, $\alpha_b = N/(M + N)$.

The good agreement of the CTMA exponents with their exact values over the complete range of n_d for the single-channel model and in the Kondo regime of the multi-channel model may be taken as evidence that the T-matrix approximation correctly describes both the FL and the non-FL regimes of the $SU(N) \times SU(M)$ Anderson model ($N=2$, $M=1,2,4$). The static spin susceptibility χ of the single- and of the two-channel Anderson model in the Kondo regime calculated within CTMA as the derivative of the magnetization $M = \frac{1}{2}g\mu_B \langle n_{f\uparrow} - n_{f\downarrow} \rangle$ with respect to a magnetic field H is shown in Fig. 5. Good quantitative agreement with exact solutions is found for $N = 2$, $M = 1$ (FL). For $N = 2$, $M = 2$ (NFL) CTMA correctly reproduces the exact [25] logarithmic temperature dependence below

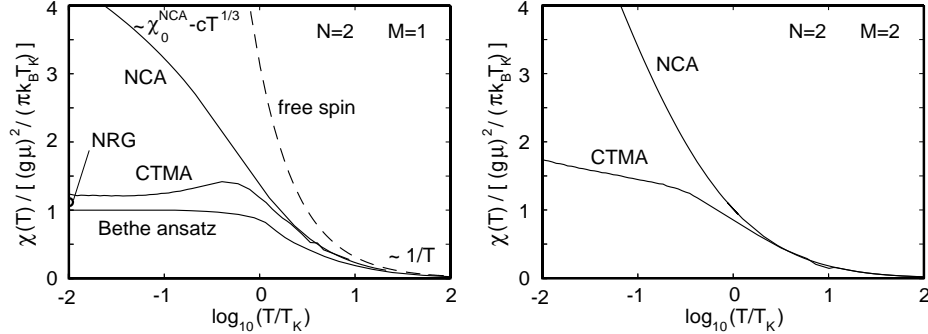


Figure 5 Static susceptibility of the single-channel ($N = 2$, $M = 1$) and the two-channel ($N = 2$, $M = 2$) Anderson impurity model in the Kondo regime ($E_d = -0.8D$, $\Gamma = 0.1D$, Landé factor $g = 2$). In the single-channel case, the CTMA and NCA results are compared to the NRG result ($T = 0$, same parameters) [23] and to the Bethe ansatz for the Kondo model [24]. The CTMA susceptibility obeys scaling behavior in accordance with the exact results (not shown).

the Kondo scale T_K . In contrast, the NCA solution recovers the logarithmic behavior only far below T_K .

4 Conclusion

We have reviewed a novel technique to describe correlated quantum impurity systems with strong onsite repulsion, which is based on a conserving formulation of the auxiliary boson method. The conserving scheme allows to implement the conservation of the local charge Q without taking into account time dependent fluctuations of the gauge field λ . By including the leading infrared singular contributions (spin flip and charge fluctuation processes), physical quantities, like the magnetic susceptibility, are correctly described both in the Fermi and in the non-Fermi liquid regime, over the complete temperature range, including the crossover to the correlated many-body state at the lowest temperatures. As a standard diagram technique this method has the potential to be applicable to problems of correlated systems on a lattice as well as to mesoscopic systems out of equilibrium via the Keldysh technique.

We wish to thank S. Böcker, T.A. Costi, S. Kirchner, A. Rosch, A. Ruckenstein and Th. Schauerte for stimulating discussions. This work is supported by DFG through SFB 195 and by the Hochleistungsrechenzentrum Stuttgart.

Bibliography

- [1] A. C. Hewson, *The Kondo Problem to Heavy Fermions* (C.U.P., Cambridge, 1993).
- [2] For a comprehensive overview see D. L. Cox and A. Zawadowski, *Adv. Phys.* **47**, 599 (1998).
- [3] W. Metzner and D. Vollhardt, *Phys. Rev. Lett.* **62**, 324 (1989).
- [4] A. Georges et al., *Rev. Mod. Phys.* **68**, 13 (1996).
- [5] For an overview and references see, e.g., *Quantum dynamics of submicron structures*, H. A. Cerdeira, B. Kramer and G. Schön, eds., NATO ASI Series E **291** (Kluwer, 1995).
- [6] D. C. Ralph et al., *Phys. Rev. Lett.* **72**, 1064 (1994).
- [7] S. E. Barnes, *J. Phys.* **F6**, 1375 (1976); **F7**, 2637 (1977).
- [8] A. A. Abrikosov, *Physics* **2**, 21 (1965).
- [9] P. Coleman, *Phys. Rev.* **B29**, 3035 (1984).
- [10] G. Baym and L.P. Kadanoff, *Phys. Rev.* **124**, 287 (1961); G. Baym, *Phys. Rev.* **127** 1391 (1962).
- [11] P. Nozières and C. T. De Dominicis, *Phys. Rev.* **178**, 1073; 1084; 1097 (1969).
- [12] P. W. Anderson, *Phys. Rev. Lett.* **18**, 1049 (1967).
- [13] K. D. Schotte and U. Schotte, *Phys. Rev.* **185**, 509 (1969).
- [14] B. Menge and E. Müller-Hartmann, *Z. Phys.* **B73**, 225 (1988).
- [15] J. Kroha, P. Wölfle and T. A. Costi, *Phys. Rev. Lett.* **79**, 261 (1997).
- [16] For a more detailed discussion see J. Kroha and P. Wölfle, *Acta Phys. Pol. B* **29**, 3781 (1998); cond-mat# 9811074.
- [17] T.A. Costi, P. Schmitteckert, J. Kroha and P. Wölfle, *Phys. Rev. Lett.* **73**, 1275 (1994); *Physica (Amsterdam)* **235-240C**, 2287 (1994).
- [18] S. Fujimoto, N. Kawakami and S.K. Yang, *J.Phys.Korea* **29**, S136 (1996).
- [19] I. Affleck and A.W.W. Ludwig, *Nucl. Phys.* **352**, 849 (1991); **B360**, 641 (1991); *Phys. Rev. B* **48**, 7297 (1993).
- [20] N. Grewe and H. Keiter, *Phys. Rev. B* **24**, 4420 (1981).
- [21] Y. Kuramoto, *Z. Phys. B* **53**, 37 (1983); Y. Kuramoto and H. Kojima, *ibid.* **57**, 95 (1984); Y. Kuramoto, *ibid.* **65**, 29 (1986).
- [22] D. L. Cox and A. E. Ruckenstein, *Phys. Rev. Lett.* **71**, 1613 (1993).
- [23] We are grateful to T. A. Costi for providing the NRG data.
- [24] N. Andrei, K. Furuya, J.H. Löwenstein, *Rev.Mod.Phys.* **55**, 331 (1983).
- [25] N. Andrei, C. Destri, *Phys. Rev. Lett.* **52**, 364 (1984).